The "U-Tube": An Improved Aspirated Temperature System for Mobile Meteorological Observations, Especially in Severe Weather

SEAN M. WAUGH[a]

[a] *NOAA/OAR National Severe Storms Laboratory, Norman, Oklahoma*

(Manuscript received 29 January 2021, in final form 18 June 2021)

ABSTRACT: Obtaining quality air temperature measurements in complex mesoscale environments, such as thunderstorms or frontal zones, is problematic and is particularly challenging from a moving platform. For some time, mobile weather platforms known as mobile mesonets (MMs) have used custom aspirated temperature shields. The original design was known as the "J-tube," which addresses some but not all of the unique problems associated with mobile temperature measurements. For VORTEX2 2009, a second, well-documented shield, the R.M. Young (RMY) 43408, was included but was also found to have certain shortcomings in some severe weather environments. Between the end of VORTEX2 2009 and the start of VORTEX2 2010, a third and new shield called the "U-tube" was designed, tested, and installed. Reported here are the results of efforts to better characterize the J-Tube, RMY 43408, and U-tube. Several tests designed to isolate key aspects of a radiation shield's performance, such as performance in rain, high solar radiation, varying wind conditions, and general response time, were completed. A period of intercomparison among the three shields during the 2010 season of VORTEX2 is also used to highlight each shield being used in "real world" conditions. Results indicate that the U-tube has several significant advantages over the J-tube and 43408 in terms of aspiration rate, sampling efficiency, performance during rain, variable winds, and high solar radiation periods, as well as response time. Given these results, the U-tube should be utilized for mobile observations going forward.

SIGNIFICANCE STATEMENT: Observations of the atmosphere are a critical component of research, particularly that involving severe weather. Errors, biases, and incorrect readings of these observations can cause problems during analysis or lead to incomplete or even incorrect conclusions. Radiation shields used for temperature observations are used to protect sensors but can have a significant effect on the observations themselves. Older radiation shields such as the "J-tube" are shown here to have some potential problem areas when using them to house temperature sensors. A new shield, the "U-tube," has been created to mitigate these effects and to provide a functional radiation shield capable of performing in a wide range of conditions, from severe weather (thunderstorms, hurricanes, etc.) to more calm weather.

KEYWORDS: Storm environments; Surface temperature; In situ atmospheric observations; Instrumentation/sensors; Measurements; Surface observations

1. Introduction

It is no surprise that in situ surface observations have been, and continue to be, an important aspect of a variety of field work efforts to understand the environment around us, including a wide range of mesoalpha, beta, and even microscale phenomena. The level of detail required however, is often difficult to achieve with stationary sites due to site spacing, network location, and probability of encountering an event of interest (Trapp 2013). An alternate approach is to use a network of mobile platforms with similar observational capabilities as a stationary site, for example, a "mobile mesonet" (MM; Straka et al. 1996). The MMs were originally a joint venture between the University of Oklahoma School of Meteorology, the Cooperative Institute for Mesoscale Meteorological Studies (CIMMS), and the National Severe Storms Laboratory (NSSL). Since its original inception in the Verification of Rotation in Tornadoes Experiment (VORTEX) in 1994 (Rasmussen et al. 1994), the MM system (and the concept of a mobile weather station) has become widely accepted and has been used or copied, in part or in whole, for a number of field projects spanning a wide range of conditions (Rasmussen et al. 1994; Straka et al. 1996; Buban et al. 2007; Markowski 2002a,b, 2002; Lang et al. 2004; Pietrycha and Rasmussen 2004; Shabbott and Markowski 2006; Grzych et al. 2007; Stonitsch and Markowski 2007; Hirth et al. 2008; Kosiba et al. 2013) and from a variety of groups (Karstens et al. 2010; Taylor et al. 2011; Skinner et al. 2011; Lee et al. 2011; Richardson et al. 2010).

The original MM was mounted on a 1993 Chevy Corsica (Fig. 1), and made basic observations of temperature, pressure, wind speed/direction, relative humidity (RH), and location (Straka et al. 1996). Given that the original version of the MM was created nearly 25 years ago, it is an understatement to say that there have been significant changes/modifications to the overall design and operating characteristics of the MM platform. This is particularly relevant with regard to the solar radiation shield commonly known as the "J-tube" that was used during the original VORTEX project.

While a comprehensive review of the entire updated MM system is saved for a follow-up article, this study explores the efficiency and accuracy of the J-tube and an in-house radiation

Corresponding author: Sean M. Waugh, sean.waugh@noaa.gov

DOI: 10.1175/JTECH-D-21-0008.1

FIG. 1. NSSL Mobile Mesonet during the original VORTEX field project.

shield specifically designed for use in severe weather. Furthermore, the concept of a response "system" is explored with regard to temperature observations so that a more complete understanding of how temperature observations are made can be gained. Error sources are explored and an analysis of the performance characteristics of several radiation shields is presented. Section 2 describes the history and background of several radiation shields as well as some difficulties associated with making mobile temperature observations. Sections 3 lays out the framework of several key tests designed to explore the effectiveness of a radiation shield and examine the results. Section 4 summarizes the results and makes a recommendation for a radiation shield to be used going forward.

2. Background

a. Challenges of mobile observations

When making mobile temperature observations, there are a host of influences that can lead to errors in the collected data. While it is not always possible to eliminate or otherwise account for all error sources, knowing under what conditions they occur is paramount. Any user of observational data should understand the limitations of the observation platform and recognize where potential problem areas exist and be critical of all data collected. An individual radiation shield is designed to perform in a specific set of conditions, for example, in direct sunlight where solar radiation errors can be high. Using a radiation shield outside of these intended conditions can lead to measurement error. Even in the presence of significant errors, data can *look real* and plausible.

With that in mind, there are a few general considerations that should be given to radiation shields to be used in mobile applications.

1) HAZARDOUS WEATHER

Observational platforms that are intended to be used in severe weather events must be able to withstand the severe weather hazards (such as hail) that accompany those environments. This certainly includes the observational vehicle itself (e.g., the windshield), but this is particularly relevant for sensors and observational equipment that can break and/or perform poorly because of damage. Breakage of temperature shields or other sensors when encountering large hail [greater than 2 in. (5.08 cm) in diameter] results in lost or compromised data as well as an increase in operational costs and down time due to maintenance efforts. If mobile platforms are moving, it adds to the impact speed of any hail that is present. Any system on a mobile platform used in these conditions must be able to resist impact damage from a range of objects, such as hail, rocks, debris, or low tree branches. This adds a layer of requirements to designing observational systems for mobile vehicles that is not typically present on stationary sites.

In addition to the frequent occurrence of hail, severe weather can often be accompanied by severe winds. Observational platforms used in these settings need to be able to accurately collect representative data in a large range of flow conditions. As the vehicle itself can move, these conditions can be encountered on even quiescent days (e.g., highway speeds can produce $+35\,\mathrm{m\,s^{-1}}$ flow over the vehicle). These conditions can change rapidly as the vehicle moves through the environment, creating nearly stationary conditions above the vehicle at any speed, changing directions relative to the vehicle, or even adding to the forward motion of the vehicle for higher flow conditions. It is also important to note that these flow conditions can be modified by the vehicle itself. Thus, it is imperative that radiation shields in use on a mobile platform operate as intended in a range of relative wind directions and speeds.

2) RAIN

Rain, a common occurrence with thunderstorms, can also lead to air modification from shield surfaces through wet-bulb effects. Ambient air passing over any wetted surface on its way

to the temperature sensor will be adversely modified by evaporational cooling and significant (in both amplitude and duration) errors can occur (Lenschow and Pennell 1974; Heymsfield et al. 1979; Lawson and Cooper 1990; Eastin et al. 2002; Houston et al. 2016). The larger the upstream surface, the more ''wetted'' these surfaces can become. When combined with larger aspiration rates and lower environmental humidity, large wet-bulb errors can occur over a longer period of time. Stacked pie plates and louvered shield designs are particularly susceptible to this problem due increased surface area in high relative winds that can force water inside the shield (Straka et al. 1996). Furthermore, mobile platforms exacerbate the problem as they move in and out of rain or road spray environments rapidly and repeatedly. Radiation shields should minimize these effects by isolating sensors from liquid precipitation and shedding excess water efficiently.

3) SOLAR RADIATION

Previous studies of temperature shield performance have specifically focused on the negative effects of solar radiation during low wind conditions (Brasefield 1948; Fuchs and Tanner 1965; Hubbard et al. 2004). Reradiation of energy absorbed by nearby surfaces can lead to modification of ambient air parcels and result in errors of the measured temperature, thus most temperature shields are designed to minimize the exposed surface the measured air must pass over.

Many commercially available radiation shields are designed to shield the installed temperature sensors from incoming solar radiation by covering the sensor from above. To maintain a quick response to changes in ambient temperature, these sensors are generally exposed from below. Over grassy terrain or soil, this works reasonably well as radiation reflected off the surface is generally minimal. Higher aspiration rates (either through a fan or by relative winds) can reduce this effect, but placement over a vehicle provides yet another challenge with direct solar energy that is reflected.

Windshields or the typically reflective, glossy paint of vehicle surfaces can redirect incoming solar radiation back toward an exposed temperature sensor much the same way snow over open terrain can. It is typically assumed that black paint can reduce this effect by absorbing rather than reflecting some of the incoming energy. This absorbed energy, however, leads to increased thermal energy in a surface and transfers to nearby air parcels, biasing temperature observations. White surfaces would reduce this thermal adsorption but are typically more reflective and can increase the total solar radiation on a surface from nontypical angles, resulting in observational errors (Richardson et al. 1999). In short, a temperature shield must be able to reflect or redistribute energy caused by strong solar radiation from a large range of incoming angles.

4) RESPONSE TIME

For a given sensor, the amount of time it takes to register and respond to a change is generally known as its response time or time constant. This is typically specified under some specific condition by the instrument manufacturer, but in practical application the response time of a sensor is dynamic, changing significantly depending on the evolving conditions around it. The phrase ''time constant'' is therefore incorrect, as it implies an unchanging value. Response time is a much more appropriate description. Rather than focusing on the factory specified response time of a sensor, however, it is important to take in to account the response time of the complete ''system.'' Here, ''system'' implies, for example, the temperature sensor and all the shield components and characteristics together, as every piece contributes to the system's effective response time. This concept applies to any sensor in use but is particularly applicable to temperature observations. For example, a system consisting of a temperature sensor in a shield with low aspiration would have an increased effective time constant relative to the same sensor in a shield with higher aspiration.

The temperature of upstream thermal mass can modify the measured air prior to reaching the sensor (Fuchs and Tanner 1965) and can also result in an increase in the effective response time. Even filters covering the sensor membrane for protection, such as with combination temperature and RH (T/RH) probes, can alter the measured values (Richardson et al. 1998). The factory-specified response time for these sensors may not take these effects into account and may not be as reliable as an absolute value.

The response time of the system directly affects the interpretation of data collected. The system response time, measured as the response to a step change, has the effect of being a ''gradient dampener'' in practical applications. Transient meteorological temperature features will be smoothed from their full value, potentially to the point of being indistinguishable from background noise, by sensor systems with effective response times too long. The accuracy of the sensor is *irrelevant* if the system response time is inappropriate for the time scales of variations being studied.

Since mobile platforms can pass through temperature features at high speeds, the temperature system must be designed so that changes are measured quickly (e.g., having a high degrees Celsius per second). Because the platform is moving however, the vehicle speed translates this temporal response into a spatial one (e.g., degrees Celsius per kilometer). Having a slower response means the system takes longer in time and space to register the same changes as a faster system. For example, if we assume a 5°C step change and a system response time of 10 s, a MM traveling at 20 m s^{-1} would sample the boundary at approximately 15.8°C km^{-1}. The same system traveling at 40 m s^{-1} would only sample 7.9°C km^{-1} during the same time period. A longer response time and/or a fast vehicle motion can smooth out gradients and make features appear much broader spatially than in reality. For a spatially narrow feature, a slowly responding system combined with a fast vehicle motion could result in dampening the feature to the point of being indistinguishable.

5) EXTERNAL INFLUENCES

In addition to the factors listed already, mobile observations provide a unique and challenging external influence source that can further complicate observations: namely, that the observation platform itself produces heat and follows other platforms that do the same. The vehicle engine produces heat as the vehicle runs, which is directed under and over the vehicle

to help to prevent the engine from overheating. This heated air can significantly bias observations if the modified air is ingested into an observing system. If there are other vehicles present on a roadway (a common occurrence during operations), the modified air from their engines can also affect observations. Heavy traffic or following closely behind another vehicle can create a persistent bias in temperature observations, while lighter traffic can cause shorter-duration errors. The number of vehicles, the types of vehicles present (both from traffic and the observational platform itself), following distance, wind direction/speed, and vehicle motion can all influence the degree to which these influences are present.

Radiation shields should be able to adequately mix environmental air to avoid continued bias and should be mounted in a location to reduce the likelihood that modified air is ingested. In situations in which an observational vehicle is following closely behind traffic, there is typically not much that can be done to reduce the observational errors as the entire airstream can be biased relative to the ambient environment, but it is important to recognize these periods when they occur and exclude them from analysis.

b. *Radiation shields*

To make effective and accurate observations of T/RH, the sensors themselves must be placed in a shield to reduce negative influences such as rain and solar radiation on the sensors. This shield is an integral part of a T/RH observing system and affects all aspects of the accuracy and representativeness of those observations as previously discussed. Too often manufacturer-specified accuracy and response time is interpreted as system accuracy and response time. A fast responding sensor in a poorly designed radiation shield can be less effective than a slower responding sensor in a better radiation shield.

Given the propensity of the NSSL MMs to operate in severe thunderstorm environments, it has been found that commercially available shields are not adequate for operations. The design and lightweight materials often used do not stand up to repeated exposure to high wind environments typical on a moving platform, or encounters with even moderately sized hail. Thus, a need exists for a shield capable of making observations in and around severe weather that is capable of withstanding the typical environments being sampled. However, the MMs are capable of sampling a variety of conditions and are used in data collection during nonsevere weather events as well. Thus, the radiation shield in use by the NSSL MMs should be versatile and perform in a wide range of conditions.

1) THE J-TUBE RADIATION SHIELD

To meet this need, a custom-made shield known as the ''J-tube'' was created for the original VORTEX project (Fig. 2; Straka et al. 1996). For a bit of context, the J-tube more closely resembles an ''S'' shape. However, the design itself was created by Dr. Jerry Straka and was affectionately called the ''J-tube'' in his honor. Largely made from polyvinyl chloride (PVC), the J-tube was modeled after a reverse-flow temperature sensor for aircraft, which requires the airstream to make several sharp turns, mechanically separating liquid water and reducing wet-bulb errors (Rodi and Spyers-Duran 1972). For this feature to work properly, the J-tube must always be pointing ''into the wind,'' and the exhaust portion of the J-tube must be located in the accelerated airstream immediately above the roof of the vehicle (Fig. 3). Houston et al. (2016) also show this accelerated airstream in their computational fluid dynamics (CFD) wind-tunnel simulation of a recently retired minivan version of the MM to determine how the vehicle itself was (potentially) modifying observations. The installation practice of the J-tube induces a pressure gradient force across the intake and exhaust, which draws air through the system. A small direct current (DC) fan is also located in the exhaust to draw air through whenever the ambient wind is calm.

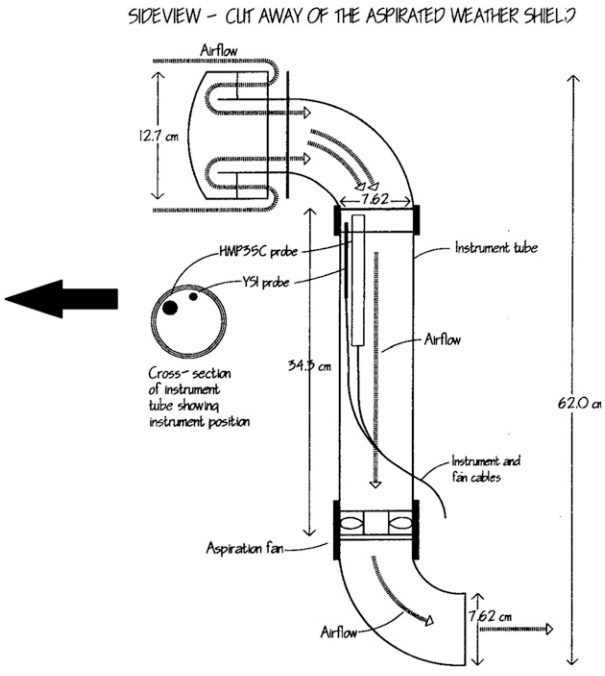

FIG. 2. Side view of the J-tube design, indicating airflow patterns, measurements, and sensor location. The thick arrow indicates the direction of the vehicle nose. Proper installation direction can be noted in Fig. 1 [this figure is adapted from Straka et al. (1996)].

Limited testing was done on the J-tube to verify its functionality prior to being put into operational use (this can be explained by the fact that the J-tube was created mere days before the start of the original VORTEX project). As such there are several questions with regard to the J-tube's ability to perform in regions of high solar radiation or changing wind conditions, or its overall effectiveness at representing sharp gradients in the natural environment.

2) THE R.M. YOUNG MODEL 43408

Because of the relative unknowns with the J-tube, it was determined that the J-tube alone would not be suitable for all possible MM applications in the 2009 season of VORTEX2. To address this issue, an R.M. Young Model 43408 Gill Aspirated Radiation Shield (Fig. 4; hereinafter referred to simply as the 43408) was added to the MM rack in addition to the J-tube. This shield is commonly used on stationary networks and is

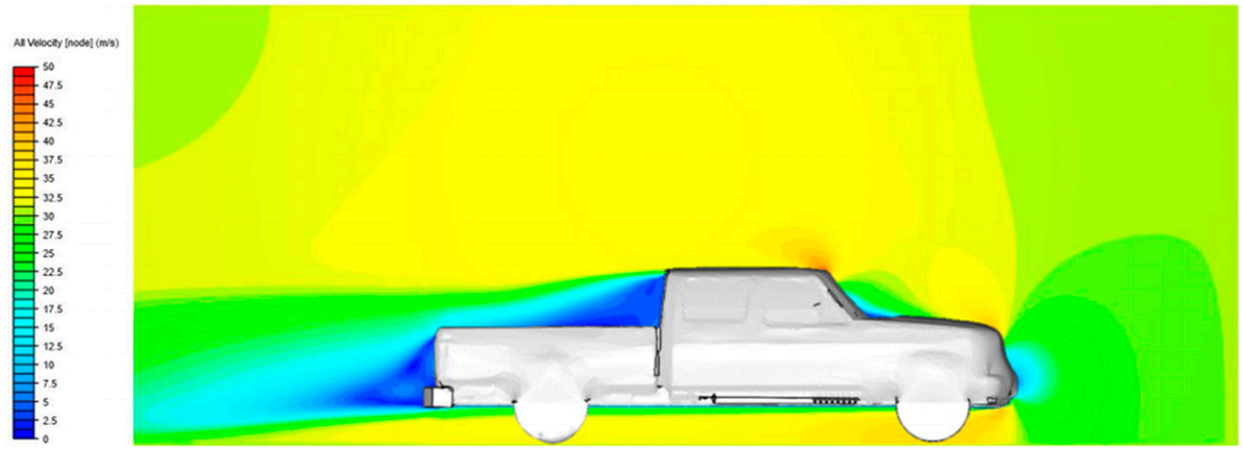

FIG. 3. Side view of Ford F350 pickup truck with flow distortion from 30 m s^{-1} forward motion visualized. Yellow colors indicate flow >30 m s^{-1}, an acceleration over the ambient flow rate.

considered to be a reference during periods of high solar radiation (Richardson et al. 1999; Anderson and Baumgartner 1998; Hubbard et al. 2004; Brandsma and van der Meulen 2008). It was not, however, intended to be used on a mobile platform and has no documentation about changes in the ambient wind speed/direction and their effect on the aspiration rate of the unit. In addition, Brandsma and van der Meulen (2008) noted a tendency for the 43408 to experience wet-bulb errors during periods of rain. These errors require further exploration.

3) THE U-TUBE RADIATION SHIELD

Given that both the J-tube and the 43408 contain uncertainties, and the hypothesis that neither shield would be fully adequate in its capability to observe a wide range of environmental conditions, a third shield was designed. The ''U-tube'' was designed to provide robust observations of T/RH in a large variety of conditions (Fig. 5). This shield takes after the J-tube in that it requires airflow to make an upward turn against gravity to enter the unit, thereby mechanically separating liquid water. The sensors are housed in the horizontal section, with the intake featuring a stacked double plate arrangement with a smaller diameter inner tube that extends from the intake to just before the sensors. This arrangement provides an insulating corridor of air inside the U-tube, allowing excess heat absorbed by the exterior and transferred to the interior air to be ducted away. The air entering the intake comes from underneath the bottom plate, minimizing surfaces over which it passes before entering the shield and reducing both wet-bulb and solar radiation errors. The exhaust portion of the U-tube contains a small DC fan, similar to the J-tube, to aspirate the unit in the absence of environmental flow. The primary aspirating mechanism, however, is through a pressure gradient force caused by the curved plate mounted above the flat plate. This arrangement accelerates the airflow between the plates and produces a low pressure within the exhaust, thus drawing air in the intake and through the shield. Both the intake and the exhaust are symmetrical, reducing dependencies on ambient wind direction. This is similar in function to the J-tube but does not require the presence of the accelerated airflow from a vehicle to function. An example installation location of the U-tube is shown in Fig. 6 on a mobile mesonet in use during a field project in 2019.

The intention of the U-tube was to provide a durable, omnidirectional, Bernoulli enhanced temperature shield that protected installed sensors from solar radiation and rain, while

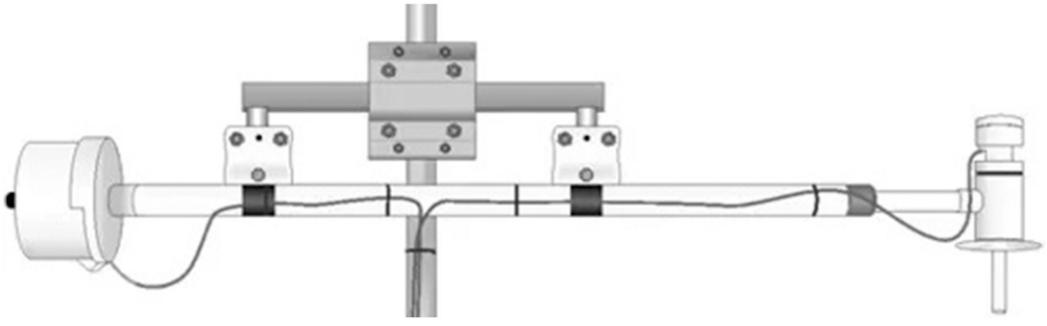

FIG. 4. Side view of the R.M. Young Co. model 43408. The intake is the downward pointing assembly on the right, with the exhaust fan located in the box assembly on the left.

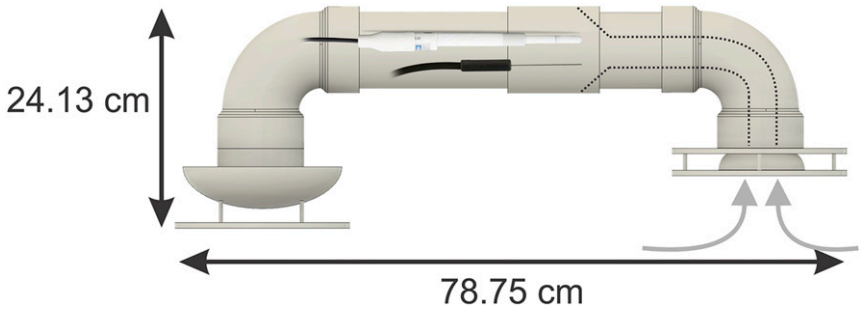

FIG. 5. U-tube schematic showing dimensions (cm) and airflow patterns (gray-filled arrows). Black dotted lines indicate interior tubing/structure. The U-tube is made from a combination of thin- and thick-walled schedule-40 PVC and uses a small DC fan in the exhaust (0.85 $m^3 min^{-1}$) to help to aspirate the unit in low wind conditions. The unit is intended to be mounted horizontally as shown, with the intake (right) and the exhaust (left) pointing downward toward the surface. Example instruments (HMP155 and 109ss) are shown in their mounting location.

maintaining positive flow rates in a variety of conditions. Utilizing the features of the design, the shield should maintain adequate exchange rates between the sensors and the outside air, as well as increase the ambient airflow rate as the vehicle travels at increasing speeds. More details on the construction of the U-tube can be found in Waugh (2012).

3. Performance testing

When evaluating any instrument system, it is imperative to understand the limitations of the system as a whole. Knowing the response characteristics, and more importantly when problems are likely to occur, is critical to working effectively with any data collected. To explore the effectiveness of the J-tube, the U-tube, and the 43408 on a mobile platform, a series of tests were performed that isolated a number of key influences on each system and compared their results.

Note that these tests and evaluations were performed by attempting to isolate specific conditions with real data. In an ideal world, putting the *entire* MM in a wind tunnel with precise wind, pressure, humidity, and temperature control as well as the ability to introduce rain would be the best method for robustly determining the operating characteristics of the entire system. In practice, however, a wind tunnel of that size is neither available to nor cost-effective for the author for the purposes of this study. Additionally, the author is not aware of a wind tunnel with all of the abovementioned controls. Given this situation, controlled, isolated tests focusing on specific aspects of the system were used to observe the performance characteristics of each shield.

a. Solar radiation

To determine the sensitivity of either the J-tube or the U-tube to incoming solar radiation, a metal halide lamp was used to mimic solar heating (McPherson et al. 2007) from a variety of angles relative to the intake portion of each radiation shield. Given that both the J-tube and the U-tube are unknowns, the 43408 radiation shield was used as a reference (Richardson et al. 1999; Anderson and Baumgartner 1998; Hubbard et al. 2005; Brandsma and Vander Meulen 2008). The 1000 W lamp produced an equivalent of 950 W m^{-2} at a distance of approximately 0.787 m over a circular area of approximately 0.381 m in diameter and was assumed to be uniform. Each of the three radiation shields used a Thermometrics (TMM) T5503 temperature sensor (±0.15°C accuracy). In each setup, 0°, 45°, and 90° angles were used from both front facing and from the side of the intake portion of each radiation shield, with each run lasting 30 mins and 0° being a horizontal solar angle. This process effectively simulated a number of potential solar angles likely to be experienced. The maximum deviation from the reference of each run is shown in Table 1.

In general, the U-tube responded better through the variety of solar angles than the J-tube. On average, the U-tube deviated from the 43408 reference by 0.5°C, whereas the J-tube experienced a roughly 1°C deviation. This can likely be attributed to the large PVC cap on the intake of the J-tube, which can absorb incoming solar energy and transfer that energy to environmental air passing over it on its way to the internal sensors. This is reflected in the maximum deviations occurring at 0° relative to the intake. Previous tests of the J-tube presented by Straka et al. (1996) showed a slightly better performance of the J-tube when compared with Oklahoma Mesonet (OM) sensors (an improvement of ~1°C). It is important to note, however, that the OM radiation shield at the time was unaspirated, and temperature errors in excess of 1°–2°C are common (Hubbard et al. 2001) for unaspirated shields and can be significantly higher. Additionally, the sun angle was relatively high and wind speeds relatively low, creating poor conditions for unaspirated shields and arguably better conditions for the J-tube. Furthermore, no information about the degree of incoming solar radiation is provided. Thus, the results presented here are in line with those presented previously for the J-tube, albeit more comprehensive. Conversely, the U-tube has minimal surfaces over which the sampled air passes, thus reducing the effects of solar radiation. Furthermore, while there are external surfaces of the U-tube that are heated and transfer energy to air internally, this air is ducted away from the sensor to further minimize solar radiation errors.

While it is useful to examine the maximum deviations in Table 1, the rate at which each shield began to show a

FIG. 6. A mobile mesonet vehicle in use during the Target Observations by Radars and Unpiloted Aerial Systems (UAS) in Supercells (TORUS) project in 2019. The U-tube can be seen on the front portion of the instrument rack, mounted above the front end of the truck.

deviation is also important. The J-tube began to show increased air temperatures within roughly 5 min of the solar lamp being applied (not shown). Conversely the U-tube took nearly 15–20 min before showing a noticeable increase in temperature. With such a quick response, the J-tube will begin to show solar radiation bias in even relatively short bursts of direct solar radiation. These finding represent a worst case scenario, one in which there is strong solar insolation and no ambient wind. In the case where ambient wind is present, some of this excess heating will be advected away from the intake, resulting in lower total error.

b. Precipitation

Given that the NSSL MMs core mission involves observations in severe weather, it is imperative that any shield be able to reduce wet-bulb effects during precipitation events. If liquid water is allowed to reside on shield surfaces, or be ingested into the shield itself, significant temperature errors can occur as discussed in section 2a(2). While the J-tube was designed predominantly after an aircraft shield intended to reduce these effects, neither it or the U-tube or the 43408 have been explicitly tested in precipitation events. The most direct way of evaluating a radiation shields performance during rain, is to put it into rain. Given that the U-tube, the J-tube, and the 43408 were all in use on each vehicle during the 2010 season of the VORTEX2 project, there are multiple cases that can be examined with the collocated sensors to identify periods of precipitation and any potential errors. A case from 10 May 2010 is examined here (Fig. 7).

Between 2100 and 2315 UTC, the MM was being driving in dry, cloudy conditions. All three shields (the U-tube, J-tube, and 43408) agree within the uncertainty limit of the sensors. At approximately 2315 UTC, the MM was driven into a brief heavy rain event that lasted until roughly 2345 UTC. During this time, all three radiation shields showed a cooling relative to the prerain environment as expected; however, the 43408 showed a significant deviation of nearly −2°C during this time. The 43408 is particularly susceptible to errors during precipitation as the sensor is located very close to the opening of the intake, allowing water to easily be ingested and collected on the sensor surface. The behavior has been visually observed on numerous occasions. Once the rain ceases, the excess water is shed and the 43408 returns to agreement with the J-tube and U-tube. A second and longer period of rain was encountered

TABLE 1. Solar radiation–induced temperature errors (°C) for the U-tube and J-tube after a 30-min exposure to 950 W m^{-2} solar radiation as compared with the 43408. The value shown is the maximum difference achieved.

Orientation; angle	U-tube difference (°C)	J-tube difference (°C)
Front; 0°	0.5	1
Front; 45°	0.3	0.7
Front; 90°	0.5	0.7
Side; 0°	0.6	1.1
Side; 45°	0.4	0.8
Side; 90°	0.5	0.7

shortly after 0000 UTC 1 May and shows deviations for both the 43408 and the J-tube (−3° and −1°C, respectively) from the observed U-tube temperature. The prolonged period of rain encountered here allowed water to eventually work its way into the J-tube, which is likely a combination of duration and changing wind conditions.

Thus, both the 43408 and the J-tube are likely to encounter errors when used in heavy precipitating events. Note that this does not mean that the U-tube is "error free," simply that it was the least affected between the three shields. As drop size distributions tend toward smaller diameter drops, liquid water will be drawn into temperature systems as small drops more closely follow the airstream. This is particularly problematic in road spray conditions when following vehicles on wet roadways with droplet sizes approaching that of mist, which tends to follow airstreams more closely. During these conditions, it is expected that nearly any radiation shield would ingest liquid precipitation. With heavier rain events while precipitation is actively falling, it can generally be assumed that the wet-bulb temperature and air temperature are relatively close, minimizing evaporative cooling errors. Water can linger on roadways well after precipitation has ended however, leading to potential sources of error. Furthermore, these conditions can change rapidly and are therefore difficult to quantify. Data in these regions should be flagged for examination.

c. *Wind direction and speed*

On a mobile platform, the relative wind that a given shield experiences is a combination of the vehicle motion as well as the ambient environmental motions. This relative wind can have significant influences on the aspiration of the shield itself, which can slow, stall, or even reverse the intended flow direction and lead to potential errors. To test the response of both the J-tube and the U-tube to changing wind directions, each shield was mounted on the MM on an adjustable arm that allowed the unit to be rotated relative to the nose of the vehicle. All shield orientations, for both the J-tube and the

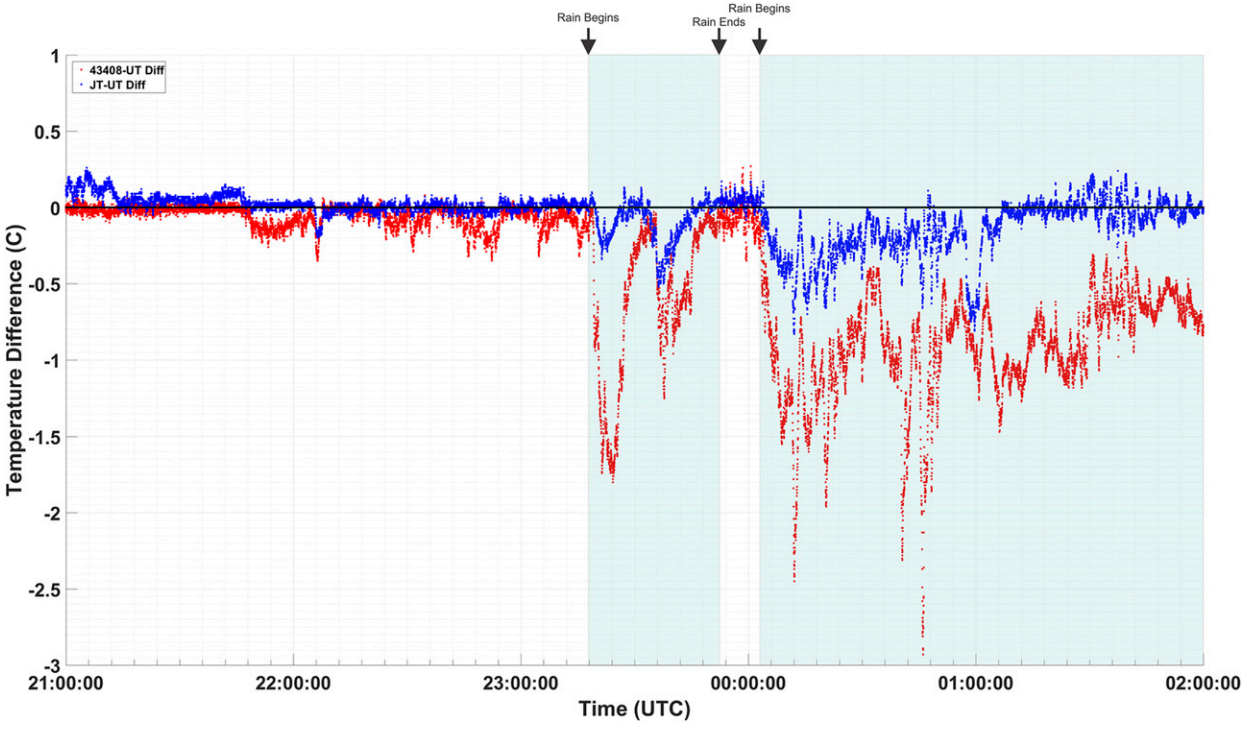

FIG. 7. Temperature difference for Probe 2 during VORTEX2 on 10 May 2010 between the J-tube and U-tube (blue) and the 43408 and the U-tube (red). In both cases the U-tube is considered the reference and is subtracted from the other to highlight periods during which the 43408 or J-tube show lower temperatures (i.e., a negative deviation) relative to the U-tube. The black line indicates zero. The data collection period is characterized by several periods of rain (2320–2345 and 0000–0130 UTC, marked by arrows and shaded sections) during which the 43408 shows colder temperatures than either the J-tube or the U-tube. At the beginning of the period, before the rain events, all three systems agree to within the specifications of the sensors.

U-tube, were performed with the radiation shields mounted well above the accelerated airflow of the vehicle. This was done intentionally to isolate the shields from any external effects (such as vehicle influences) and test only the base response of the system. The MM was then driven at night down a straight, flat, semirural road with no ditches and little traffic during calm conditions to recreate a controlled relative wind over the vehicle, simulating a variety of wind directions relative to the shield body. Doing so reduced potential turbulent effects from passing vehicles or convective cells off the roadway due to solar heating, which could cause localized fluctuations in the ambient wind. This process was repeated at 4.5, 8.9, 17.9, and 26.8 $\mathrm{m\,s^{-1}}$ vehicle speeds and at shield rotation angles of 45°, starting with 0°, which corresponds to the native orientation of each shield. To measure the internal flow in each of the shields, a Thermo Systems, Inc., (TSI) Model 8455–06 hot-wire anemometer was used. The low profile of this device minimized flow distortion inside the shield and allowed the aspiration rate to be measured near the temperature sensing elements. The mean flow rates for both the U-tube and J-tube under varying vehicle speeds and rotation angles is shown in Fig. 8, with standard error of the distribution shown as error bars.

It is important to reiterate that this test removed the J-tube from its traditionally installed location directly above the roof of the vehicle, which was its intended location when originally designed. This was done intentionally to observe the characteristics of the shield itself outside of any external influence. Placement over a vehicle will affect the performance of the J-tube (which was the original intent) and is exceedingly specific to individual vehicles. Because of the currently wide use of the J-tube on a variety of vehicles and in a variety of mounting locations, an understanding of the base state operation is needed. For reference, in calm conditions the J-tube maintains a roughly 2.5 $\mathrm{m\,s^{-1}}$ flow rate, whereas the U-tube maintains approximately 5 $\mathrm{m\,s^{-1}}$ flow.

In the figure, the U-tube (solid lines) maintains a relatively constant flow rate between 5 and 10 $\mathrm{m\,s^{-1}}$ despite changing relative flow conditions. As the wind speed over the U-tube increases, so does the internal aspiration. The minimum flow rate of 5 $\mathrm{m\,s^{-1}}$ is held by the small DC fan located in the exhaust portion of the structure. Conversely the J-tube (dashed lines) shows a significant dependency on both wind speed and direction. With the wind direction positioned toward the front of the J-tube (270°–0°–90° relative to the intake), there is minimal deviation in the internal aspiration rate of the J-tube. However, as the wind direction shifts toward the rear of the J-tube there is a large dependency on the relative wind speed. In all tested wind speeds the flow reverses direction when the J-tube relative wind direction has a rearward component, reaching a maximum of $-13\ \mathrm{m\,s^{-1}}$ for the 26.8 $\mathrm{m\,s^{-1}}$ case.

Given this behavior, the J-tube is not well suited for observations in conditions where the relative wind may shift the angle of attack. The reverse-flow design being modeled after an aircraft design makes the assumption that the relative flow will *always* be toward the nose of the J-tube. While this is *likely* during mobile operations, it is not a guarantee as high environmental winds can offset even fast vehicle motions. Reversing flow inside the radiation shield can lead to additional errors as heat from the DC fan, the vehicle body, or rain is ingested into the system. Additionally, flow can stagnate, leading to a decoupling from the ambient environment. Even in cases in which the relative wind is from the front of the J-tube, the aspiration rate remaining constant despite increases in the relative wind speed effectively increases the response time of the system as a whole (as opposed to the U-tube, which increases its aspiration). Hypothetically, as a vehicle travels forward at increasing speeds, the J-tube is cycling air inside the system at the same rate. This behavior would tend to drag out any changes sampled by the moving platform and decrease the effectiveness of the J-tube as a radiation shield. While a faster fan could be used to reduce this behavior and increase the base aspiration rate of the system, doing so would only shift the sensitivity slightly higher and not high enough to remove the potential for negative flow conditions. A fan to completely negate the possibility of negative flow is not practical given the size and power requirements of the J-tube. Installing the J-tube with the exhaust in an accelerated airflow [as intended in the original Straka et al. (1996) design] only shifts this response slightly and is dependent on the presence of the accelerated airflow, which is not a guarantee.

Given that the J-tube has been used extensively in past field campaigns, analysis should focus only cases in which the relative wind is from 270°–0°–90° directed toward the nose of the vehicle and has a minimum magnitude of 5 $\mathrm{m\,s^{-1}}$. This ensures that the J-tube is properly aspirating and reduces the risk of exposure errors in the reverse-flow conditions. It is important to note that these reverse-flow conditions can occur while moving, so all data points need to be examined. Conversely the U-tube is more amenable to these variable conditions with a useful response to the changing environment. While its response is not entirely symmetric (likely due to turbulence from either the exhaust or intake of the shield itself, and/or the structure on which it is mounted), the aspiration of the U-tube never decreases below its nominal value.

As a point of discussion, there is no clear answer as to a target aspiration rate that is desirable or required for temperature systems. The requirements for aspiration can vary significantly from one project to the next and between systems. At a minimum, the aspiration of a radiation shield should be positive in all cases and maintain at flow rate of at least 5 $\mathrm{m\,s^{-1}}$. This ensures that the sensors inside are properly ventilated at all times and keeps with the relative historical context of other sensors (e.g., radiosondes typically ascend at this speed and several commercial radiation shields have aspiration rates between 5 and 8 $\mathrm{m\,s^{-1}}$). This is a subjective target, however, as different systems may require different aspiration rates. It is critically important to understand the relationship between the aspiration rate of a radiation shield and its response time, which will be explored further in section 4.

d. System response time

A final benchmark for the performance of a T/RH shield is to understand the system response characteristics to an impulse change in the ambient environment. This response time is critical to assessing how quickly a system will respond to a change in temperature. While accuracy is important, if the *system* takes too long to reach sufficiently close to a final

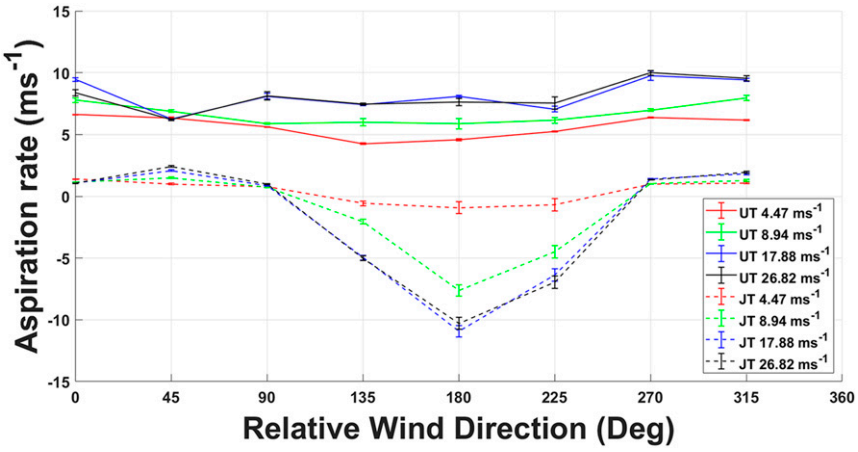

FIG. 8. Sensitivity of the U-tube's (solid) and J-tube's (dashed) mean flow rate to varying relative wind direction angles (horizontal axis) at 4.47 (red), 8.94 (green), 17.88 (blue), and 26.82 (black) m s^{-1} wind speeds. Error bars represent the standard error of the sample. Graph indicates the J-tube's sensitivity to the relative wind and its tendency to decrease its flow rate to the point of reversing directions when the flow approaches the rear of the J-tube.

temperature, then the final conditions may change before the correct observation is taken, rendering the system inaccurate. While a complete characterization of the temperature system is impossible as there are an infinite number of changing conditions that cannot be observed at all times, a baseline comparison is useful to determine how the systems compare on an ''even playing field.''

To test the base response time of each temperature system, a cart-mounted version of the MM rack with the J-tube, U-tube, and 43408 installed was put through a step change in temperature. A cart mounted rack was used to more readily facilitate a rapid change in temperature when moving the instruments between environments. For the test, all three radiation shields had identical TMM T5503 temperature sensors installed to maintain comparability. In addition, the U-tube and the J-tube had HMP35 T/RH probes installed as they are commonly used for temperature observations. The NSSL vehicle bay was utilized for this purpose during the winter months as it is heated, providing a sharp gradient between the interior and exterior environments. The test was completed by moving the cart from inside the vehicle bay to outside the garage door as rapidly as possible. It was completed at night, during calm wind conditions, to minimize influences from solar radiation and turbulence, and ensure that the aspiration through each system was due only to that systems fan rather than any ambient flow conditions present.

The response time of each shield is found, following Brock and Richardson (2001), by

$$x(t) = x_{FS} - (x_{FS} - x_{IS})e^{-t/\tau}, \quad (1)$$

where x_{IS} is the initial state, x_{FS} is the final state, t is time, $x(t)$ is the system temperature at time t, and τ is the time constant of the system. If the initial and final states are known, and t is set to τ, Eq. (1) can be solved to determine the value of $x(t)$ after the response time of the system has passed following a step change. An examination of the data, and the amount of time required to reach this temperature, yields the response-time value. In practical terms, this value is the time it takes to reach 63% (1/e, where e is the natural number 2.718 28) of the total change in temperature experienced.

During the test, each of the three systems had significantly different responses to the same step change in temperature (Fig. 9). During the experiment, the initial state was 20.5°C and the final state was 2.5°C, an 18°C step change (simulated by the solid red line in Fig. 9). Following the method outlined in Eq. (1), $x(t)$ = 9.2°C when $t = \tau$, which took 76 s for the TMM sensor in the J-tube to reach (Fig. 9, orange line). Similarly, the same sensor in the U-tube (Fig. 9, yellow line) and the 43408 (Fig. 9, purple line) required only 33 and 18 s, respectively.

The 43408 is clearly the faster-responding system in these conditions. Errors in excess of 3°C, 17% of the step-change magnitude, occurred between the J-tube and the U-tube simply because of their response-time differences when comparing individual points. Furthermore, the temperature sensor inside the HMP35 sensors for both the J-tube (green line) and the U-tube (blue line) were considerably slower, 5 min 16 s and 4 min 28 s, respectively. This indicates that while the HMP35 combination T/RH sensor is needed for dewpoint observations, the response of the system to changes in temperature is too slow for any practical use in environments where temporal changes are at time scales typical in mesoscale sensing. Note that the overall magnitude of error that can occur due to a lagged response is proportional to the magnitude of the step change, with larger steps producing more significant deviations for slower systems.

It is worth reiterating that the numbers quoted above are from a single trial and are not necessarily constant and should not be treated as such. There are a variety of factors that can and will change from moment to moment that influence the observations taken. The shock experiment was repeated 4 times, at varying temperature differences to determine if there were radical changes that occurred from one run to the next. Table 2 shows the average, maximum, and minimum

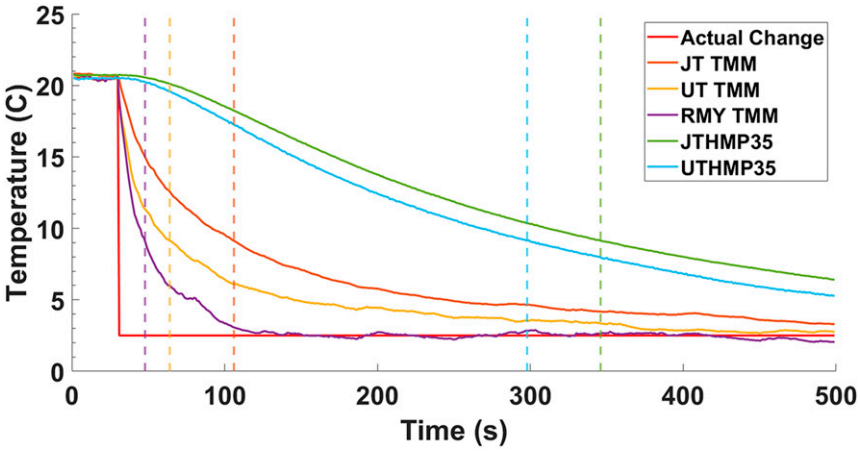

FIG. 9. Step change in temperature for the cart-mounted MM rack with an initial temperature of 20.5°C and a final temperature of 2.5°C (red). The J-tube TMM (dark orange), U-tube TMM (light orange), 43408 TMM (purple), J-tube HMP35 (green), and U-tube HMP35 (blue) are also shown in solid lines. Dashed vertical lines of each color represent the effective response time of each respective sensor.

response times over the four trials done for each sensor. The 43408 is remarkably consistent, which given the short path to the sensor is to be expected. The U-tube and J-tube both showed a range of roughly 20 s, though the U-tube is below the J-tube in both range and average value. It is worth noting, however, that the best performance of the J-tube is comparable to the worst performance of the U-tube. The HMPs were slightly less variable in either shield, with the exception of a single trial for the U-tube, which produced the outlier of 268 s, with the remainder of the trials tightly clustered around 160 s.

The difference in response times between the three systems is entirely based on the radiation shields themselves as each system had identical sensors. The physical mass of each radiation shield has its own temperature in a given environment and will tend toward the ambient temperature after a change, albeit at a slower rate. Any mass upstream of a sensor will impart its temperature onto the air prior to sampling, thereby modifying the responsiveness of the system. The amount of mass upstream, the speed of air passing over it, and even the material the shield is made from all contribute to rate of transfer to the sampled air. The 43408 has very little in the way of upstream thermal mass ahead of the sensor and utilizes lightweight plastic with a low capacity for heat storage as well as a relatively fast aspiration rate ($8\ m\ s^{-1}$), leading to a faster response time for a given change. The J-tube has a large PVC cap on the intake that has a large capacity to store heat and a low aspiration rate (maximum of $5\ m\ s^{-1}$), leading to sampled air having an increased contact time with surfaces and more potential for modification. The U-tube has a reduced thermal mass relative to the J-tube, though not as much as the 43408, and therefore has a response time between the two.

4. Conclusions

With the results in section 3, it is evident that the J-tube's design makes it sensitive to changes in the relative wind, while its slow response time can alter the appearance of any temperature gradients sampled. Any true environmental change observed by the J-tube would have a lower maximum magnitude and would be drawn out over an extended period of time, misrepresenting the true environmental change. This gradient dampener could drastically misrepresent observational gradients critical to the study of complex problems such as boundary interactions in tornadic supercells. Additionally, its use in situations involving high values of solar radiation results in errors, which was cautioned against by Straka et al. (1996). Ultimately, the J-tube's design and response characteristics make it a poor choice when considering a T/RH shield for a wide range of applications. The U-tube does not have these directional sensitivities and is much faster to respond to changes in temperature while simultaneously reducing errors associated with solar radiation.

The 43408 works well during most nonsevere conditions and has an advantage in base response time over the U-tube and J-tube, as well as being a standard in high solar radiation, but shows deficiencies in severe weather conditions typical of MM operation. Wet-bulb errors are common during rain events and its susceptibility to hail makes the unit's use in convective weather research problematic at best. Furthermore, since the 43408 does not alter its aspiration rate positively with changes in the relative wind, it will be slower to mix the ambient air at high relative winds speeds while driving down the road. In this

TABLE 2. Range of response times for various shock tests performed.

Sensor	Avg (s)	Max (s)	Min (s)
J-tube TMM	66.5	76	52
U-tube TMM	44	52	34
43408 TMM	16	18	13
J-tube HMP35	323.5	336	311
U-tube HMP35	191	268	164

regard, the U-tube alleviates these problems by increasing its mixing rate with increasing relative wind speed as well as being directionally insensitive.

Overall, the U-tube represents a compromise in the typical operating conditions for a mobile platform to maximize its applicability across a wide range of conditions. Its design allows the system to be responsive while minimizing errors from environmental influences. Furthermore, the ability of the U-tube to operate independently of the vehicle flow as is the case with the J-tube, allows the U-tube to be mounted higher and farther forward on an observational rack. This can act to reduce the influence of engine heat from the vehicle during operations by placing the unit outside of the typical path of this airstream. This makes the U-tube a more robust choice when designing a mobile observation platform for scientific measurements. If used together, the J-tube and the 43408 could conceivably cover most commonly encountered situations but would require the use of two shields to accomplish the same task. Furthermore, determining which shield to use in which set of conditions would be time consuming, tedious, and complicated. The authors therefore recommend that the U-tube be used from this point forward for mobile temperature measurement application. Several research institutions, including NSSL, the University of Nebraska (Houston et al. 2016), and the Center for Severe Weather Research are already utilizing the U-tube.

Acknowledgments. The basis for this research formed the author's master's thesis in 2012, and as such it had several notable influences on it. Doctors Michael Biggerstaff, Petra Klein, and Jerry Straka at the University of Oklahoma served on the author's committee during that time, and their guidance and feedback on the U-tube are greatly appreciated. Sherman Fredrickson also played a pivotal role in the development of the U-tube, with multiple conversations about design options and iterations and suggestions for various testing mechanisms. Sherman was, and continues to be, an amazing mentor and helped me to discover a passion for observational meteorology. The author also thanks Dr. Erik Rasmussen for his review of the initial draft of this paper and thanks as well the reviewers during the publication process. Funding was provided by NOAA/National Severe Storms Laboratory and by the NOAA/Office of Oceanic and Atmospheric Research under NOAA–University of Oklahoma Cooperative Agreement NA11OAR4320072, U.S. Department of Commerce, and the University of Oklahoma because the author was a student at the time of the original work.

Data availability statement. Both unique experimental data and field project data are used to explore the various aspects of the U-tube and other radiation shields for viability testing. All data used for this study are available upon request (Waugh 2020).

REFERENCES

Anderson, S. P., and M. F. Baumgartner, 1998: Radiative heating errors in naturally ventilated air temperature measurements made from buoys. *J. Atmos. Oceanic Technol.*, **15**, 157–173, https://doi.org/10.1175/1520-0426(1998)015<0157:RHEINV>2.0.CO;2.

Brandsma, T., and J. P. van der Meulen, 2008: Thermometer screen intercomparison in De Bilt (the Netherlands)—Part II: Description and modeling of mean temperature differences and extremes. *Int. J. Climatol.*, **28**, 389–400, https://doi.org/10.1002/joc.1524.

Brasefield, C. J., 1948: Measurement of air temperature in the presence of solar radiation. *J. Meteor.*, **5**, 147–151, https://doi.org/10.1175/1520-0469(1948)005<0147:MOATIT>2.0.CO;2.

Brock, F. V., and S. J. Richardson, 2001: *Meteorological Measurement Systems.* Oxford University Press, 290 pp.

Buban, M. S., C. L. Ziegler, E. N. Rasmussen, and Y. P. Richardson, 2007: The dryline on 22 May 2002 during IHOP: Ground-radar and in situ data analyses of the dryline and boundary layer evolution. *Mon. Wea. Rev.*, **135**, 2473–2505, https://doi.org/10.1175/MWR3453.1.

Eastin, M. D., P. G. Black, and W. M. Gray, 2002: Flight-level thermodynamic instrument wetting errors in hurricanes. Part I: Observations. *Mon. Wea. Rev.*, **130**, 825–841, https://doi.org/10.1175/1520-0493(2002)130<0825:FLTIWE>2.0.CO;2.

Fuchs, M., and C. B. Tanner, 1965: Radiation shields for air temperature thermometers. *J. Appl. Meteor.*, **4**, 544–547, https://doi.org/10.1175/1520-0450(1965)004<0544:RSFATT>2.0.CO;2.

Grzych, M. L., B. D. Lee, and C. A. Finley, 2007: Thermodynamic analysis of supercell rear-flank downdrafts from project ANSWERS. *Mon. Wea. Rev.*, **135**, 240–246, https://doi.org/10.1175/MWR3288.1.

Heymsfield, A. J., J. E. Dye, and C. J. Biter, 1979: Overestimates of entrainment from wetting of aircraft temperature sensors in cloud. *J. Appl. Meteor.*, **18**, 92–95, https://doi.org/10.1175/1520-0450(1979)018<0092:OOEFWO>2.0.CO;2.

Hirth, B. D., J. L. Schroeder, and C. C. Weiss, 2008: Surface analysis of the rear-flank downdraft outflow in two tornadic supercells. *Mon. Wea. Rev.*, **136**, 2344–2363, https://doi.org/10.1175/2007MWR2285.1.

Houston, A. L., R. J. Laurence III, T. W. Nichols, S. Waugh, B. Argrow, and C. L. Ziegler, 2016: Intercomparison of unmanned aircraft-borne and mobile mesonet atmospheric sensors. *J. Atmos. Oceanic Technol.*, **33**, 1569–1582, https://doi.org/10.1175/JTECH-D-15-0178.1.

Hubbard, K. G., X. Lin, and E. A. Walter-Shea, 2001: The effectiveness of the ASOS, MMTS, Gill, and CRS air temperature radiation shields. *J. Atmos. Oceanic Technol.*, **18**, 851–864, https://doi.org/10.1175/1520-0426(2001)018<0851:TEOTAM>2.0.CO;2.

——, ——, C. B. Baker, and B. Sun, 2004: Air temperature comparison between the MMTS and the USCRN temperature systems. *J. Atmos. Oceanic Technol.*, **21**, 1590–1597, https://doi.org/10.1175/1520-0426(2004)021<1590:ATCBTM>2.0.CO;2.

Karstens, C. D., T. M. Samaras, B. D. Lee, W. A. Gallus, and C. A. Finley, 2010: Near-ground pressure and wind measurements in tornadoes. *Mon. Wea. Rev.*, **138**, 2570–2588, https://doi.org/10.1175/2010MWR3201.1.

Kosiba, K., J. Wurman, Y. Richardson, P. Markowski, P. Robinson, and J. Marquis, 2013: Genesis of the Goshen County, Wyoming, tornado on 5 June 2009 during VORTEX2. *Mon. Wea. Rev.*, **141**, 1157–1181, https://doi.org/10.1175/MWR-D-12-00056.1.

Lang, T. J., and Coauthors, 2004: The Severe Thunderstorm Electrification And Precipitation Study. *Bull. Amer. Meteor. Soc.*, **85**, 1107–1125, https://doi.org/10.1175/BAMS-85-8-1107.

Lawson, R. P., and W. A. Cooper, 1990: Performance of some airborne thermometers in clouds. *J. Atmos. Oceanic Technol.*, **7**, 480–494, https://doi.org/10.1175/1520-0426(1990)007<0480:POSATI>2.0.CO;2.

Lee, B. D., C. A. Finley, and T. M. Samaras, 2011: Surface analysis near and within the Tipton, Kansas, tornado on 29 May 2008. *Mon. Wea. Rev.*, **139**, 370–386, https://doi.org/10.1175/2010MWR3454.1.

Lenschow, D. H., and W. T. Pennell, 1974: On the measurement of in-cloud and wet-bulb temperatures from an aircraft. *Mon. Wea. Rev.*, **102**, 447–454, https://doi.org/10.1175/1520-0493(1974)102<0447:OTMOIC>2.0.CO;2.

Markowski, P. M., 2002a: Hook echoes and rear-flank downdrafts: A review. *Mon. Wea. Rev.*, **130**, 852–876, https://doi.org/10.1175/1520-0493(2002)130<0852:HEARFD>2.0.CO;2.

——, 2002b: Mobile mesonet observations on 3 May 1999. *Wea. Forecasting*, **17**, 430–444, https://doi.org/10.1175/1520-0434(2002)017<0430:MMOOM>2.0.CO;2.

——, J. M. Straka, and E. N. Rasmussen, 2002: Direct surface thermodynamic observations within the rear-flank downdrafts of nontornadic and tornadic supercells. *Mon. Wea. Rev.*, **130**, 1692–1721, https://doi.org/10.1175/1520-0493(2002)130<1692:DSTOWT>2.0.CO;2.

McPherson, R. A., and Coauthors, 2007: Statewide monitoring of the mesoscale environment: A technical update on the Oklahoma mesonet. *J. Atmos. Oceanic Technol.*, **24**, 301–321, https://doi.org/10.1175/JTECH1976.1.

Pietrycha, A. E., and E. N. Rasmussen, 2004: Finescale surface observations of the dryline: A mobile mesonet perspective. *Wea. Forecasting*, **19**, 1075–1088, https://doi.org/10.1175/819.1.

Rasmussen, E. N., J. M. Straka, R. Davies-Jones, C. A. Doswell, F. H. Carr, M. D. Eilts, and D. R. MacGorman, 1994: Verification of the Origins of Rotation in Tornadoes Experiment: VORTEX. *Bull. Amer. Meteor. Soc.*, **75**, 995–1006, https://doi.org/10.1175/1520-0477(1994)075<0995:VOTOOR>2.0.CO;2.

Richardson, S. J., S. E. Fredrickson, F. V. Brock, and J. A. Brotzge, 1998: Combination temperature and relative humidity probes: Avoiding large air temperature errors and associated relative humidity errors. Preprints, *10th Symp. on Meteorological Observations and Instrumentation*, Phoenix, AZ, Amer. Meteor. Soc., 6–14.

——, F. V. Brock, S. R. Semmer, and C. Jirak, 1999: Minimizing errors associated with multiplate radiation Shields. *J. Atmos. Oceanic Technol.*, **16**, 1862–1872, https://doi.org/10.1175/1520-0426(1999)016<1862:MEAWMR>2.0.CO;2.

Richardson, Y. P., P. M. Markowski, S. Waugh, and S. Fredrickson, 2010: Mobile mesonet observations in VORTEX2. *25th Conf. on Severe Local Storms*, Denver, CO, Amer. Meteor. Soc., P6.4, https://ams.confex.com/ams/25SLS/webprogram/Paper176206.html.

Rodi, A. R., and P. A. Spyers-Duran, 1972: Analysis of time response of airborne temperature sensors. *J. Appl. Meteor.*, **11**, 554–556, https://doi.org/10.1175/1520-0450(1972)011<0554:AOTROA>2.0.CO;2.

Shabbott, C. J., and P. M. Markowski, 2006: Surface in situ observations within the outflow of forward-flank downdrafts of supercell thunderstorms. *Mon. Wea. Rev.*, **134**, 1422–1441, https://doi.org/10.1175/MWR3131.1.

Skinner, P. S., C. C. Weiss, J. L. Schroeder, L. J. Wicker, and M. I. Biggerstaff, 2011: Observations of the surface boundary structure within the 23 May 2007 Perryton, Texas, supercell. *Mon. Wea. Rev.*, **139**, 3730–3749, https://doi.org/10.1175/MWR-D-10-05078.1.

Stonitsch, J. R., and P. M. Markowski, 2007: Unusually long duration, multiple-Doppler radar observations of a front in a convective boundary layer. *Mon. Wea. Rev.*, **135**, 93–117, https://doi.org/10.1175/MWR3261.1.

Straka, J. M., E. N. Rasmussen, and S. E. Fredrickson, 1996: A mobile mesonet for finescale meteorological observations. *J. Atmos. Oceanic Technol.*, **13**, 921–936, https://doi.org/10.1175/1520-0426(1996)013<0921:AMMFFM>2.0.CO;2.

Taylor, N. M., and Coauthors, 2011: The Understanding Severe Thunderstorms and Alberta Boundary Layers Experiment (UNSTABLE) 2008. *Bull. Amer. Meteor. Soc.*, **92**, 739–763, https://doi.org/10.1175/2011BAMS2994.1.

Trapp, R. J., 2013: *Mesoscale-Convective Processes in the Atmosphere.* 1st ed. Cambridge University Press, 400 pp.

Waugh, S., 2012: The ''U-Tube'': An improved aspirated temperature system for mobile meteorological observations, especially in severe weather. M.S. thesis, School of Meteorology, College of Atmospheric and Geographic Sciences, University of Oklahoma, 76 pp., https://shareok.org/handle/11244/24679?show=full.

——, 2020: The ''U-Tube'': An improved aspirated temperature system for mobile meteorological observations especially in severe weather. NOAA/NSSL, accessed 30 July 2020, https://data.nssl.noaa.gov/thredds/catalog/PARR/2020/Sean-Waugh/The-U-Tube:-An-improved-aspirated-temperature-system-for-mobile-meteorological-observations-especially-in-severe-weather.html.